

Comparative Study of Some Atmospheric Transmittance Indices over JOS Using Recurrence Quantification Analysis

O. V. EDWARD¹, O. R. OBASI-OMA²

¹(Department of Physics, Federal University of Technology, Akure, Ondo state, Nigeria)

²(Department of Physics, Federal University of Technology, Akure, Ondo state, Nigeria)

Corresponding Author: O. V. EDWARD

Abstract: Solar radiation at the earth's surface is essential for the development and utilization of solar energy. It is needed for designing collectors for the solar heater and other photovoltaic equipment that depend on solar energy. Atmospheric transmittance is the capacity of the atmosphere to transmit electromagnetic energy. Analysis of direct, diffuse radiation and clearness index is needed to approximate the amount of solar energy availability. In this study, Satellite data (The Modern – Era Retrospective analysis for research and application, Version 2 (MERRA-2)) consisting of hourly global and diffuse solar radiation measured over ten (10) years, from January 2006 to December 2015 was utilized to investigate the availability and predictability of hourly clearness index (M_t), transmitting index (M_T) together with the diffuse fraction (M_d) in Jos meteorological station ($9.88^\circ N$, $8.8^\circ E$) located in Nigeria. From the phase plots, recurrence plots (RP), it was observed that M_t and M_T have low predictability during the wet season months, with high availability during the dry season months. This was further validated by using two Recurrence Quantification Analysis (RQA) measures: Determinism (DET) and Entropy (ENT). In all cases considered, it was observed that the RQA measures for M_d is very low when compared to that of M_t and M_T , with the exception of March. The information provided in this study can provide useful information about sky condition which solar energy engineers and analysts can utilize for the designing of collectors for solar heaters and other photovoltaic equipment that depends on solar energy.

Keywords-Predictability, Recurrence Quantification Analysis (RQA), Recurrence plot (RP), Solar radiation, Transmittance indices.

Date of Submission: 28-06-2019

Date of acceptance: 15-07-2019

I. Introduction

In applied dynamics, the goal is to relate mathematical systems to physical or biological systems of interest. The approach in most cases involves model building—we use our understanding of the physical system to write dynamical equations that describe the evolutionary behaviour of the system. In some cases where all one has access to is a sequence of measurements taken at some times separated at a particular interval of time, the opposite approach is taken. This approach involves starting with the sequence of measurements—a time series—and then employ some numerical or analytical tools to process the time series in order to reveal the dynamical behaviour underlying physical system being represented by the measured data. The time series can represent the measurement of the processes and dynamics of the natural system under study. In most cases it reveals the behavioral nature of the system—whether linear, periodic or quasi-periodic. Most of these processes can best be studied using the nonlinear approach (Hegger et al., 1994 and Unnikrishnan, 2010).

Solar radiation at the earth's surface is essential for the development and utilization of solar energy. It is needed for designing collectors for the solar heater and other photovoltaic equipment that depend on solar energy. Solar radiation (or short-wave radiation) is the radiation, or energy we get from the sun. It comes in many forms, such as visible light, radio waves, heat (infrared), x-rays, and ultraviolet rays and consists of the direct, diffuse and reflected radiation. It is a major driver for many physical, chemical and biological processes on earth's surface; such that the complete and accurate solar radiation data at specific regions are of great significance for researches and application fields such as architecture, industry, agriculture, environment, hydrology, meteorology, limnology, oceanography and ecology. Solar radiation data are fundamental input for solar energy applications such as photovoltaic systems for electricity generation, solar collectors for heating, solar air conditioning climate control in buildings and passive solar devices (Sopian et al., 2009).

Knowledge of the global solar radiation is of fundamental importance for all solar energy conversion systems. For effective production and prediction of solar radiation, one should be able to characterize the nature and predictability of the recorded time series of the solar radiation and the related transmittance parameters to find the proper model structure as well as the model inputs and to be able to claim the validity of its model.

One of the ways of easily estimating the incident solar radiation incident on a horizontal or inclined surface, which is a requirement for design purposes, is by establishing the sky conditions at the locality. (Ideriah and Suleman, 1989.) These conditions can be quantified by the following parameters: (i) the clearness index, $K (=H/H_0)$ (ii) the relative sunshine, $S(=N/N_0)$ (iii) the diffuse ratio or cloudiness index, $K_d(=H_d/H)$ and (iv) the diffuse coefficient, $K_{d'}(=H_d/H_0)$ (Ideriah and Suleman, 1989). Here, H represents the daily global solar radiation, H_0 the daily extraterrestrial radiation, H_d the daily diffuse radiation, N the daily sunshine duration and N_0 the maximum possible sunshine duration or daylength.

K_T gives the percentage depletion by the sky of the incoming global radiation and therefore indicates both the level of availability of solar radiation and changes in atmospheric conditions in a given locality while S is a measure of the cloud cover. K_d is the cloudiness index and $K_{d'}$ is a factor which mirrors the effectiveness of the sky in scattering the incoming radiation. These parameters have been used to establish sky conditions at various places (Liu and Jordan, 1960; Choudhury, 1963; Barbaro et al., 1981; Al-Riahi et al., 1990; Akuffo and Brew-Hammond, 1993). In Nigeria, a similar study was carried out by Ideriah and Suleman (1989) for Ibadan.

Over the years, several researches have also been carried out as regards the evaluation of the clearness index, diffuse fraction of various locations. This is because of its importance in providing useful information about the characterization of sky condition of the particular location.

Ezekwe and Clifford (1981) researched on measured solar radiation in a Nigerian environment compared with predicted data. The Diurnal global irradiation was measured with precision pyranometer in Nsukka, Nigeria and compared with values generated from five different empirical models proposed by earlier investigators. Results obtained shows that the calculated values obtained from the modified empirical formula of Swartman and Ogunlade gave the best agreement with the measured data.

Knut and Jakob (2008) carried out a study on the Transport of Solar Radiation through the Atmosphere: Aspects Relevant for Health and noted that the spectral distribution of the solar radiation reaching the Earth's surface depends on the irradiance emitted by the Sun, the Earth-Sun distance, and the transmission properties of the atmosphere. They went further to investigate the environmental effects on solar radiation transport as the absorption and multiple scattering of solar radiation determine the amount of radiation available at various levels in the atmosphere, at the surface, and at various depths in the ocean and arrived at the conclusions that changes in UV radiation exposure can be quantified and monitored, but not yet well predicted, Ozone and clouds affect the UV radiation penetration, and the cloud effect is most uncertain.

Babatunde, (2005) researched on the topic: Some solar radiation ratios and their interpretations with regards to radiation transfer in the atmosphere. The ratios of some radiation fluxes such as the global solar radiation (H), extraterrestrial solar radiation (H_0), direct solar radiation (H_b) and diffuse solar radiation (H_d) were proposed to define relevant radiation coefficients associated with the transmission of radiation in the atmosphere and the measurement of solar radiation on the ground surface. Such ratios includes: (clearness index) H/H_0 and (diffuse or cloudiness index) H_d/H was found from experiment to practically sum up to unity, i.e. $H/H_0 + H_d/H = 1$. Other ratios proposed are H_b/H , H_b/H_0 , H_d/H_0 , H_r/H_0 , and H_a/H_0 which are used to define the clearness and clearness index, transmitting coefficient, scattering coefficient, reflectance and the absorption coefficient respectively. These ratios were used to develop equations that can be used for estimating the reflection of the earth's surface and the absorption of the earth's atmosphere.

Okogbue et.al., (2009) also worked on the Hourly and daily clearness index and diffuse fraction at a tropical station, Ile-Ife, Nigeria using data from two Kipp and Zonenpyranometers models CM11 for the global radiation and CM11/121 (incorporating a shadow ring) for diffuse radiation and a LICOR LI-210SA photometric sensor for the photometric illuminance from February 1992 to December 2002. The results showed that at the station, the local sky conditions were almost void of clear skies and overcast skies. This implies that the sky conditions were rather predominantly cloudy all the year round.

Ndilemieni et.al., (2013) carried out a research work on the Evaluation of Clearness Index of Sokoto Using Estimated Global Solar Radiation. The result shows that Sokoto has a clear weather since the clearness index is more than 50% throughout the year. The month of December has the highest clearness index of 62.9% while the month of August has the least value clearness index of 50.8%. The low value of clearness index in August may be attributed to heavy rainfall associated with the month.

Yusuf, (2017) carried out a research on the Characterization of Sky Conditions Using Clearness Index and Relative Sunshine Duration for Iseyin, Nigeria. The global solar radiation, captured using Gun-Bellani distillate, calibrated in milliliter and the sunshine hours data used in this study was obtained from the archives of Nigeria Meteorological Agency (NIMET) Oshodi, Lagos, covering a period of 8 years (2000 - 2007) for the location. Result reveals that the sky conditions at Iseyin were most of time partly cloudy (partly cloudy sky occurred in eight months of the year which is about 66%. Most of these months were observed to fall in the rainy season months). Cloudy sky was only noticed in the month of August which is about 8% and it occurs at the peak of the rainy season. The region has three months of clear sky which is about 25% of the months of the

year and they are months in the Harmattan period. The prevailing sunshine condition in Iseyin is predominantly scattered clouds sky except during August and September where a cloudy sky condition was experienced.

Udo (1999) worked on Sky Conditions at Ilorin as Characterized by Clearness Index and Relative Sunshine. Here, the values of the global solar radiation (H) data were measured in accordance to the International Scale of Pyheliometry (IPS), 1977 using the Eppley Precision Spectral Pyranometer with data acquisition system, CR10 Campbell data – logger, and a storage module. The Daily sunshine duration also was measured using Campbell–Stokes recorder with heat sensitive paper. All the data covered a period of two years (i.e. September 1992 to August 1994) and the results from this work reveals that the majority of the days at the study location are relatively cloudy with hardly any very clear or overcast days. Also, the annual sky conditions have been classified into six patterns: three patterns each for the two broad seasons, dry and rainy.

Okogbue and Adedokun (2002) worked on the Characterization of sky conditions over Ile-Ife, Nigeria, based on 1992–1998 solar radiation observations. The solar radiation data used for the research work, comprising of the hourly values of both the global and diffuse solar radiation fluxes on a horizontal surface was measured, using two Kipp and Zonenpyranometers, models CM11 and CM11/121 (with shadow ring) and recorded within the ObafemiAwolowo University campus, Ile-Ife, (7.50 N, 4.50 E), Nigeria. The result shows that the annual sky conditions at the station have been shown to exhibit five characteristic patterns comprising of one distinct dry season and four distinct wet (rainy) seasons.

Many other works have been carried out to quantify sky conditions using conventional analysis, but none of these attempted to use nonlinear time series analysis tools to investigate the transmitting coefficient/ability of the atmosphere and its effectiveness in determining and defining relevant atmospheric variables in relation to radiation transfer in the atmosphere.

In this work, variation in monthlyclearness index, diffuse fraction and transmitting index (M_T , M_d and M_t respectively) were studied using recurrence plot and recurrence quantification analysis to identify periods with good and poor harvesting of solar radiation in order to provide useful information about sky condition which solar energy engineers and analysts can utilize for the designing of collectors for solar heaters and other photovoltaic equipment that depends on solar energy.

The rest of the paper is structured as follows: Section II describes the theoretical background of the study, section III describes the study area, section IV deals with the analysis of data, results and discussions, while section Vconcludes the report.

II. Theoretical Background

A.Evaluation of Some Atmospheric Transmittance Indices

The spectral distribution of radiation arriving on the earth’s surface is a function of its extraterrestrial distribution and the atmospheric constituents (Iqbal, 1983). The flux of energy received from the Sun at the horizontal surface of the atmosphere, per unit of area, at an interval of one hour (I_0) is necessary for calculation of the hourly clearness index, diffuse fraction and transmitting index (M_T , M_d and M_t) respectively. The hourly extraterrestrial solar radiation on a horizontal surface, I_0 is calculated using the expression from Iqbal (1983):

$$I_0 = I_{SC} E_0 (\sin\delta \sin\phi + \cos\delta \cos\phi \cos\omega_i) \tag{1}$$

Where I_{sc} = Solar constant ($1367W/m^2$) and E_0 = eccentricity correction factor, given as:

$$E_0 = \left(\frac{r_0}{r}\right)^2 = 1.000110 + 0.034221 \cos r + 0.001280 \sin r + 0.000719 \cos 2r + 0.000077 \sin 2 r \tag{2}$$

Γ = day angle, given as $2\pi (dn - 1)/365$ is measured in radians (3)

d_n is the day number of the year, ranging from 1 on 1st January to 365 on 31st December.

The angle of declination, δ is given as:

$$\delta = 0.006918 - 0.399912 \cos \Gamma + 0.070257 \sin \Gamma - 0.006758 \cos 2 \Gamma + 0.000907 \sin 2 \Gamma \tag{4}$$

The hourly clearness index is given by:

$$M_T = \frac{I}{I_0} \tag{5}$$

where I is the hourly global solar radiation on the horizontal surface of the earth and I_0 is the extraterrestrial horizontal radiation (measured in $KJm^{-2}h^{-1}$).

The hourly diffuse fraction on the other hand is given by

$$M_d = \frac{I_D}{I} \tag{6}$$

Also, the hourly transmitting index, M_t is given by the expression below

$$M_t = \frac{I_b}{I_0} \tag{7}$$

B. Phase space reconstruction

Phase space reconstruction is the foundation of nonlinear time-series analysis. It allows one to reconstruct the full dynamics of a complicated nonlinear system from a single time series. The standard strategy for phase space reconstruction is delay-coordinate embedding, where a series of past values of a single scalar measurement from a dynamical system are used to form a vector that defines a point in a new space.

Specifically, one constructs m-dimensional reconstruction-space vectors $\vec{P}(t)$ from m time-delayed samples of the measurements $x(t)$. The validation of the reasoning behind phase reconstruction was given by Takens theorem, (Takens, 1981), which states as follows: For a large enough embedding dimension m, the delay vectors given as

$$\vec{P}(t) = (x_t, x_{t+\tau}, \dots, x_{t+(m-1)\tau}) \quad (8)$$

yields a phase space with exactly the same invariant quantities as the original system.

where variables $x_t, x_{t+\tau}, x_{t+2\tau}, \dots, x_{t+(m-1)\tau}$ denote the values of variable x at times t, t + τ , t + 2 τ , . . . , t + (m - 1) τ with the embedding delay, τ .

There exist two methods, developed in the framework of nonlinear time series analysis that can be used to obtain the correct choice of proper embedding parameters to successfully reconstruct the phase space: the mutual information method yields an estimate for the proper embedding delay, whereas the false nearest neighbour method gives the efficient techniques to determine a proper embedding dimension. The shape of the trajectory of the reconstructed phase space gives hints about the system, and it is a starting point for further analysis and to calculate the quantifiers of the system.

C. Determination of embedding dimension and time delay

The results of nonlinear time-series analysis can be helpful in understanding, characterizing, and predicting dynamical systems. It comprises a set of methods that extract dynamical information about the succession of values in a data set. This framework relies critically on the concept of reconstruction of the phase space of the system from which the data are sampled. The theory of deterministic chaos offers an explanation for irregular behaviour of systems that are not influenced by stochastic inputs. Nonlinear time series analysis theory offers step-by-step methods that are necessary to confirm or reject the presence of deterministic chaos in a time series (Kantz and Shreiber, 2003).

i. Average Mutual Information method (AMI): Given a time series of the form $\{x_0, x_1, x_2, \dots, x_t, \dots, x_T\}$, with maximum (x_{\max}) and minimum (x_{\min}) and with absolute value of their difference $|x_{\max} - x_{\min}|$ partitioned into j equally sized intervals, where j should be a large enough integer number. Average mutual information is a popular method to find the optimum time delay (τ) required for the reconstruction of a phase space. This concept is based on information theory. The first local minima of AMI is chosen as the optimum time delay (Fraser and Swinney, 1986). It measures the extent to which $x(t + \tau)$ is related to a given τ . The mutual information can be computed using the following expression (Fraser and Swinney, 1986):

$$I(\tau) = \sum_{h=1}^j \sum_{k=1}^j P_{h,k}(\tau) \ln P_{h,k}(\tau) - 2 \sum_{h=1}^j P_h \ln P_h \quad (9)$$

where P_h and P_k denote the probabilities that the variable assumes a value inside the h-th and k-th bin, respectively, and $P_{h,k}(\tau)$ is the joint probability that x_t is in bin h and $x_{t+\tau}$ is in bin k. The embedding delay where $I(\tau)$ has the first local minimum gives the proper embedding delay.

ii. False Nearest Neighbour method (FNN)

The embedding dimension is an important parameter in the reconstruction of phase space. The dimension, in which, the attractor is unfolded need to be sufficiently large (Abarbanel et. al., 1993). This is important to remove false crossings and ensure the presence of true neighbors for every trajectory in the reconstructed phase space (Poincare, 1885). To establish a proper embedding dimension m for the examined time series, the false nearest neighbour method introduced by Kennel et al. (1992) is in most cases used. The main idea is to examine how the number of neighbours of a point change with increasing embedding dimension. The method of FNN measures the percentage of closeness, in terms of Euclidian distances, of neighboring points of the trajectory in a given dimensional space, and compares it with the next dimensional space. If the ratio of these distances is greater than a predefined threshold due to a change in the dimension, the neighbors of the trajectory are considered as false neighbors. The value of the predefined threshold should be sufficiently large so that it will allow the exponential divergence of the chaotic signal. In practice, the value of the threshold is chosen between 10 to 50 (Abarbanel et al., 1993). FNN can be computed using:

$$\left[\frac{R_{d+1}^2(t, r) - R_d^2(t, r)}{R_d^2(t, r)} \right]^{\frac{1}{2}} = \frac{|x(t + \tau) - x(t_r - \tau)|}{R_d(t, r)} > R_{tol} \quad (10)$$

where t and t_r are the times corresponding to the neighbour and the reference point, respectively. R_d denotes the distance in phase space with embedding dimension d , and R_{tol} is the tolerance threshold. Any neighbour for which equation (10) is valid is designated as FNN. The aim of the FNN method is to reduce the fraction of false nearest neighbour to the minimal.

D. Recurrence plot

Eckmann et al. (1987) elaborated graphical tools known as Recurrence Plots which are based on Phase Space Reconstruction. The recurrence plots show the time-dependent behaviour of the dynamical systems which are pictured on the phase space. A recurrence plot (RP) is a visualization of state-space dynamics that shows all those times at which a state of the dynamical system recurs.

The RP is represented as

$$R_{ij} = \Theta \left(\varepsilon_i - \left\| \vec{x}_i - \vec{x}_j \right\| \right), \quad i, j = 1, \dots, N. \quad (11)$$

where R_{ij} is the recurrence matrix, N is the number of considered states x_i , ε_i is a predefined threshold characterizing the distance between two neighbouring points, $\| \cdot \|$ a norm (i.e. Euclidean norm), Θ is the Heaviside function, \vec{x}_i and \vec{x}_j define the point in phase space at which the system is situated at times i and j respectively. A recurrence of a state at time i at a different time j is therefore marked within a two-dimensional squared matrix with ones and zeros in which axes of the recurrence matrix are time axes. One can assign "black" dot to be one and a "white" dot to be zero. A black point in the RP signifies that the system returns to an ε -neighborhood of the corresponding point in phase space (Thiel et al. 2002). The features in RP can be characterized into two patterns namely, typology (Eckmann et al. 1987) and texture Marwan (2003). For the qualitative interpretation of a RP, Marwan (2003) proposed the following guidelines which can be classified into large scale (typology) and small scale patterns (texture).

- (i) Homogeneous typologies indicates stationary.
- (ii) Fading in the upper left and lower right corners indicate nonstationarity and also contains a trend or drift.
- (iii) Disruptions (white bands) indicate that the process is nonstationarity; some states are rare or far from the normal which indicated that transitions may have occurred.
- (iv) Periodic patterns: the process gives diagonal lines and checkerboard structures; the period corresponds to the time distance between periodic patterns (e.g. lines).
- (v) For Single isolated points, the process is heavily fluctuated. If only these occur, then the process may be a random process.
- (vi) Diagonal lines (parallel with the LOI) correspond to similarities in the evolution of states at different times. The process may be regarded deterministic. if these diagonal lines are shorter, then the process can be from chaos. If the diagonals are shorter, it seems that the RP is related to the chaotic systems.
- (vii) Diagonal lines (orthogonal to the LOI) correspond to the similarities in the evolution of states at different times but they move in opposite directions in phase space. This may be a sign for an insufficient embedding.
- (viii) For Vertical and horizontal lines/clusters, system exhibiting Laminar states do not change or change slowly for some time.

E. Recurrence quantification analysis

The recurrence plot could contain hidden patterns which are not easily ascertained by visual inspection. In order to solve this problem, Zbilut and Webber (1992) proposed a tool called recurrence quantification analysis (RQA) to quantify the presence of patterns in the RPs. It quantifies the density of recurrence points as well as the histograms of the length of the diagonal and vertical lines in the RP. The measures to quantify the deterministic structure and complexity of RPs include the following:

- (i) The recurrence rate (RR) is the percentage of darkened pixels and density of recurrence points in recurrence plot.

$$RR = \frac{1}{N^2} \sum_{i,j=1}^N R_{ij} \quad (12)$$

Where N is the length of the time series and R_{ij} is recurrence matrix which is one if the state of the system at time i and that at time j have a distance less than " and zero otherwise. Its measure can be used to detect changes in a dynamical system. It values can range from 0% (no recurrence) to 100% (full recurrence).

(ii) Determinism (DET) is the ratio of recurrence points forming diagonal structures (of at least length l_{min}) to all recurrence points.

$$DET = \frac{\sum_{l=l_{min}}^N lP(l)}{\sum_{i,j=1}^N R_{ij}} \quad (13)$$

Where P(l) is the frequency distribution of the diagonal line lengths (for a diagonal parallel to the main diagonal); l is the length of the line structure. Long diagonal lines depict periodic signals (e.g. sine waves), short diagonal lines depict chaotic signals (e.g., Henon attractor) and no diagonal lines depict stochastic signals (e.g., random numbers) Webber and Zbilut (2005). It has been used successfully to quantify the degree of determinism of a physiological system

(Webber and Zbilut 1994).

(iii) Maxline (L_{max}) is the longest line segment measured parallel to the main diagonal in the plot. Eckmann et al. (1987) proposed that the longest diagonal line structure was inversely proportional to the most positive Lyapunov exponent. Trulla et al. (1996) was able to establish this for the logistic equation operating in its chaotic regime. The shorter the longest line is, the more divergent the trajectories will be. A periodic signal will give long line segments, while short lines indicate chaos.

$$DIV = \frac{1}{L_{max}}, L_{max} = \max(\{l_i; i=1, \dots, N_l\}), \quad (14)$$

N_l is the total number of diagonal lines.

(iv) Entropy (ENT) is the Shannon information entropy (Shannon 1948) of all diagonal line lengths distributed over integer bins in a histogram. It is a measure of signal complexity which shows the richness of deterministic structuring. The higher the value of Entropy, the more complex of certainty structure of the system in recurrence plot.

$$ENT = - \sum_{l=l_{min}}^N P(l) \ln P(l) \quad (15)$$

(v) Laminarity (LAM) measures the percentage of recurrent points comprising vertical line structures rather than diagonal line structures. Laminarity can vary from 0% (no laminarity) to 100% (full laminarity).

$$LAM = - \frac{\sum_{v=v_{min}}^N vP(v)}{\sum_{v=1}^N vP(v)} \quad (16)$$

Where $P(v)$ is the total number of vertical lines of the length v in the RP. Laminarity depicts the occurrence of laminar states in the system without laying emphasis on the length of these laminar phases.

III. Study Area and Method

In this study, the location under consideration is Jos meteorological station (9.88° N, 8.8°E) located in Nigeria. Nigeria is a tropical region situated between latitudes 4° and 14° North of the equator, and between longitudes 2° and 15° East of the Meridian. It experiences tropical wet and dry climates. The data used in the computations reported in this study is a Ten (10)-year (2006-2015) hourly (00:00 to 24:00 hour Local Time) satellite data of global solar radiation and diffuse solar radiation obtained from the Modern – Era Retrospective analysis for research and application, Version 2 (MERRA-2) on hourly basis.

The flux of energy received from the Sun at the horizontal surface of the atmosphere, per unit of area, at an interval of one hour (I_0) was used for calculation of the hourly clearness index, diffuse fraction and transmitting index (M_T , M_d and M_i) according to equations x, y and z respectively. The computed (M_T , M_d and M_i) were then subjected to nonlinear time series analysis. The first thing to consider in nonlinear time series analysis is the optimum values of embedding dimension (m), and delay Time (τ) (Unnikrishnan, 2010). τ was computed using the algorithm proposed by Fraser and Swinney (1986), as described in equation (9) while m was computed using the FNN method proposed by Kennel et al. (1992), as described in equation (10). The software used for all the computations, in this research work, of RP and RQA analysis is the CRP Toolbox 5.21 coded by Norbert Marwan, and freely available on the web: (<http://tocsy.pik-potsdam.de>). Details about the tool is explained in Marwan (2010).

IV. Analysis, Results and Discussions

This sections give a detailed analysis of hourly clearness index, diffuse fraction and transmitting index (M_T , M_d and M_i) data from January, 2006 to December 2015 using some nonlinear time series analysis tools.

The variations in the solar radiation, due to atmospheric dynamics, can be seen at play considering the results obtained from this work. The results obtained reveals the dynamical responses and variations in the (M_T , M_d and M_i) time series over the earth surface in Jos meteorological station.

Figure 1(a-c) represents typical plots of M_i , M_T and M_d respectively. Fluctuations displayed by different daily peaks as a result of variations in weather conditions can also be observed. The time series plots reveal possible nonlinear nature, which brings the necessity of using nonlinear time series analysis tools to quantify the availability and degree of predictability of solar radiation reception over ground surface in order to provide a useful source of information in the design and estimation of performance of solar application systems.

Considering the plot of mutual information versus time delay (τ) (Figure 2a), the corresponding value of time delay when the mutual information has its first local minimum can be chosen as the optimum value of time delay for the phase space reconstruction (Fraser and Swinney, 1986). Also, the minimal embedding dimension (m), which relates to the fraction of false nearest neighbours as shown in Figures 2b may best be defined as the embedding dimension for phase space reconstruction (Kennel et al. 1992). After further analyses, the specified $\tau \geq 8$ and $m \geq 6$ were found suitable for embedding the time series underlying M_T , M_d and M_i . However, in order not to under-embed one system than the other, the embedding dimension is chosen from a system with the higher dimension and also from the distribution of time delayed mutual information, a single value that seems to be good characterization across all the monthly data set was picked following the concept in (Wallot 2017). By repeating similar analysis for all the time series of different years considered in this study, these choices of $\tau = 8$ and $m = 7$ were found to be true. Thus, the choice of $\tau = 8$ and $m = 7$ for further analysis of this observation are reasonable.

Figures 3(a-f) present the plots for the reconstructed phase space for some selected months of the year. The 3D phase space plots were reconstructed using equation (8). It is observed for all cases, that M_i and M_T show a more deterministic structure when compared to that of M_d . The presented attractor of M_i and M_T have nice evolved folding regions, but still looks compact and deterministic. In the phase space diagram of M_d , the points are more closely packed, with high concentration in the middle of the phase space diagram. This suggest more uncertainty in the availability diffuse solar radiation in some of the seasonal months. All the phase space plots, however, do not look like a random process, rather some signature of attractor-like shape is visible in them. This observation suggests for further investigation. It was also observed that phase space cluster is usually more loosely packed from December, January and February and more closely packed during the rainy season like June, July, August and September. This might be due to the less dense atmosphere compared to the denser atmosphere on account of the reduced amount of precipitation in the dry season months. Adeyemi and Ogolo (2014) had earlier reported lower humidity in the dry seasons for some locations in West Africa. Another possible factor is the effect of aerosol loading within that region due to possible increase in these parameters in the dry season. Possible effects due to temperature gradients might also contribute greatly. During the transition months like April, October and November, the phase space trajectories look more loosely and evenly spread across the phase space.

Figure shows typical recurrence plots (RP), each representing M_i , M_T and M_d respectively. In this work, the recurrence threshold was chosen to range from 4% - 5% of the maximum attractor diameter (i.e., 8% - 10% of the corresponding attractor radius) based on the method suggested in Schinkel et al. (2008), $0.04d_A \leq \varepsilon \leq 0.05d_A$ where ε is the recurrence threshold, and d_A is the maximum attractor diameter. The method of finding the neighbours of the phase space trajectory is the euclidean norm between normalized vectors and was used throughout this study. The data used was also normalized to zero mean and standard deviation of one. The increased portion of long diagonal lines segments observed in the RPs of M_i and M_T suggests deterministic structures which are clearly visible and are interrupted by few isolated points or white horizontal and vertical spaces. (Eckmann et al. 1987, Marwan et al. 2007) while the recurrence plots for M_d looks

less densely populated with few orderly arranged parallel long diagonal lines and exhibits nonhomogeneous but quasi-periodic recurrent structures reflecting that the distances between the diagonal lines vary, and suggesting low predictability.

Since the qualitative analysis technique of the RP method is unable to give detailed information of the nonlinear dynamical system, except for the different ink (black dots) density that can only be inspected, there is a need for further analysis using RQA method. The RQA parameters such as DET, and ENT were used to further analyse the recurrence characteristics of the time series of the three atmospheric transmittance indices under consideration. The recurrence parameters were used to study the monthly variability of the data in the ten-year duration.

DET and ENT were observed to be very high at the beginning and towards the end of every year. From the beginning of the year (January) it decreases gradually towards the middle of the year (June) and rises during the short dry break between August and September known as the August break and thereafter it decreases for the remaining part of the rainy season before it rises again at the return of the dry season. Figures 5(a-e) and 6(a-e) represents the results of Determinisms for M_T and M_t in the period under investigation, while figures 8(a-e) and 8(a-e) represent the results of Entropy. For both Determinisms and Entropy, the results exhibit the same trend with high values during the dry months and low values in wet months. The measure DET shown in Figures 5 and 6 reveal the occurrence of regular patterns (predictability) in a time series for the two seasons (wet and dry seasons).

The range of the measure DET for M_t and M_T are given in Tables 1a and 1b respectively. During the ten-year duration under consideration, it can be observed that the wet (June, July and August) season months have low values of DET for M_t and M_T , while high values were observed in dry (November, December, January, February, and March) seasons.

From the sparsely populated RP in figure 4c and table 1c which shows the measure of DET for M_d , it can be observed that the contributions of diffuse solar radiation is very low throughout the years under consideration, with the exception of March, which could be as a result of presence of cloud, rainfall, suspension of water particles that lead to scattering, absorption and reflection of incoming solar radiation to the earth's surface. An increase in the entropy values at the onset of dry season was noted for the rising complexity of the deterministic part of the dynamics underlying the transmittance indices process. The high value of entropy during dry season suggests stability while the low value during wet season suggests instability. Recurrence quantification analysis has been able to reveal variability in hourly transmittance indices by high and low effect of monsoon during wet and dry seasons respectively for M_t and M_T . It is observed that the trend of DET and ENT measures follow the same trend. They decrease from a maximum in January (no rainfall) to a minimum in June/August (maximum rainfall) and therefore increase to a maximum again in December (no rainfall). In general, the similarity in the trend of DET and ENT measures might be attributed to the fact that their measurements are based on the diagonal lines of RP.

VI. Conclusion

In this research work, the evaluation of some atmospheric transmittances (clearness index, diffuse fraction and transmitting index) over Jos has been investigated using ten (10)- year satellite data of hourly global and diffuse solar radiation data obtained from Modern – Era Retrospective analysis for research and application, Version 2 (MERRA-2) from 2006-2015. Nonlinear time series analysis tools were used to analyse the data. The time delay and embedding dimension were obtained from standard algorithms, and used to draw the phase space of the time series underlying the atmospheric transmittances. Finally, RQA was used to quantify the system predictability. From the constructed phase space trajectories and the recurrence plots, it was observed for all cases, that M_t and M_T show a more deterministic structure when compared to that of M_d . The presented attractor of M_t and M_T have nice evolved folding regions and looks compact and deterministic. In the phase space diagram of M_d , the points are more closely packed, with high concentration in the middle of the phase space diagram. This suggests that solar energy devices which depends on diffuse solar radiation may not be reliable in Jos. The RQA measures (Determinism and Entropy) have high[low] values during the dry[wet] seasons. The high values of M_t and M_T recorded during the dry season months of January, February, November and December indicates that direct irradiance constitute a relatively significant proportion of the global solar irradiance reaching the ground during these months. While the low values observed for wet season months of June, July and August could be as a result of molecular scattering due to the aerosol loading of the atmosphere prevalent during this period, which is responsible for diffuse irradiance reaching the ground at these times. Also during the wet season months of July to September, the RQA measures of M_d is higher. This signifies that the high proportion of diffuse component of the total irradiance arriving on the ground during these months is as a result of the intense forward scattering of beam radiation by altocumulus and altostratus clouds (Okogbue et al., 2009). Also, the RQA measures for clearness index and transmitting index follow the same

trend in the duration under consideration. Hence, it can be deduced that just like the clearness index, the transmitting index also can be used to measure the clearness and cleanness of the atmosphere.

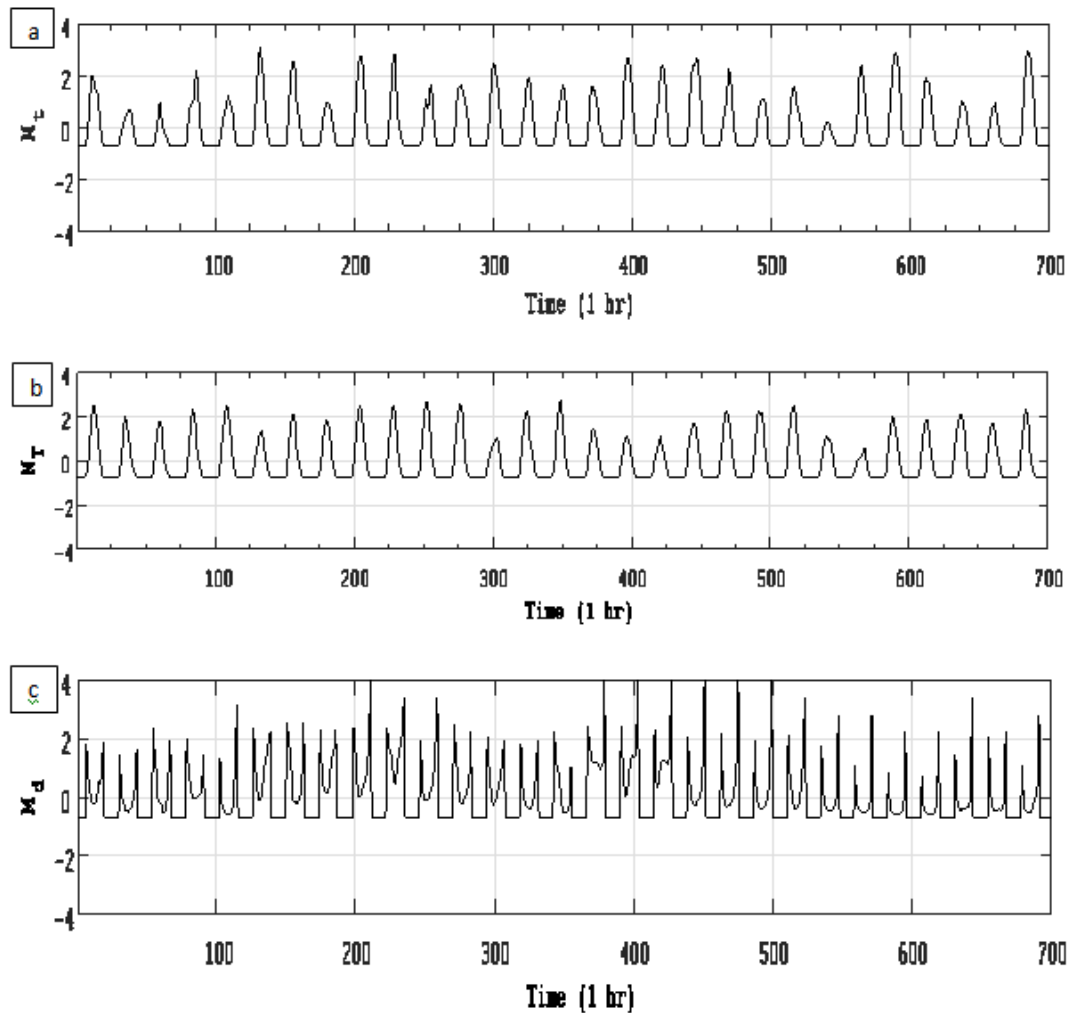
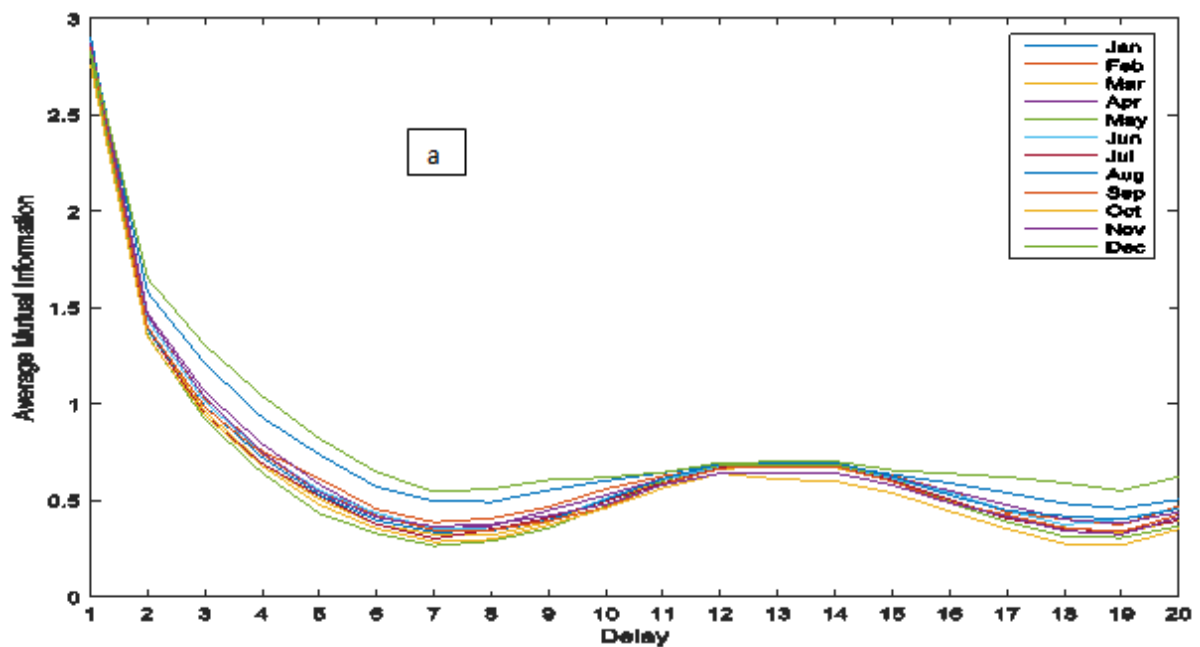


Figure 1: Typical plot of (a) M_t (b) M_T and (c) M_d in a month



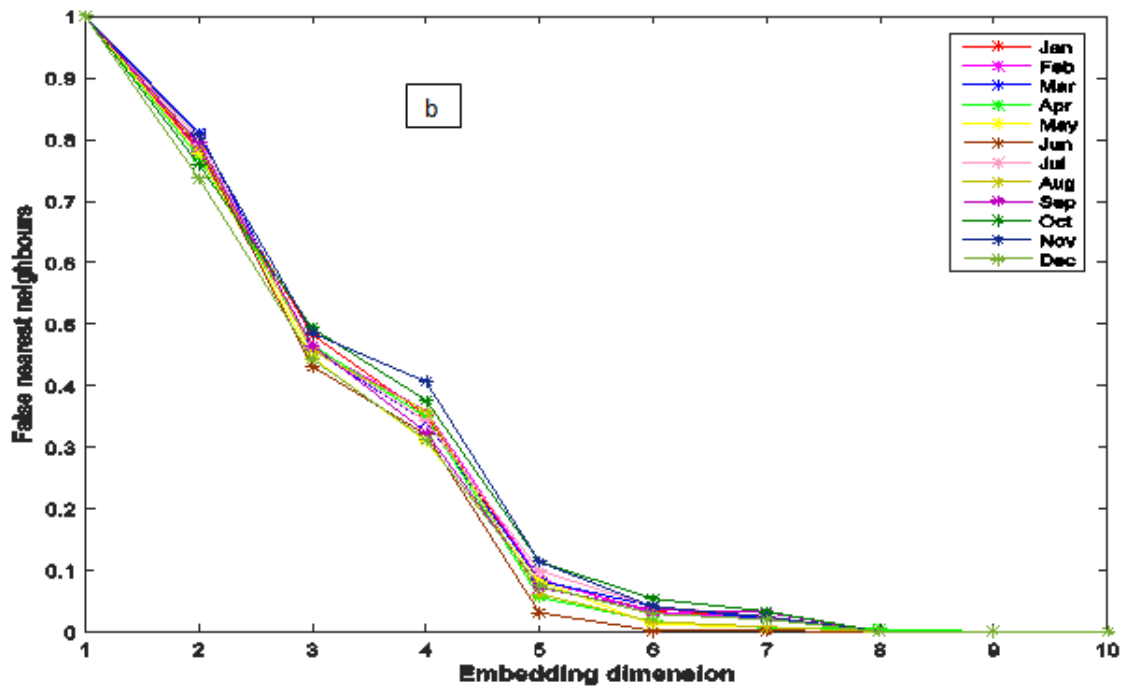


Figure 2: A typical monthly plot of (a) AMI and (b) FNN

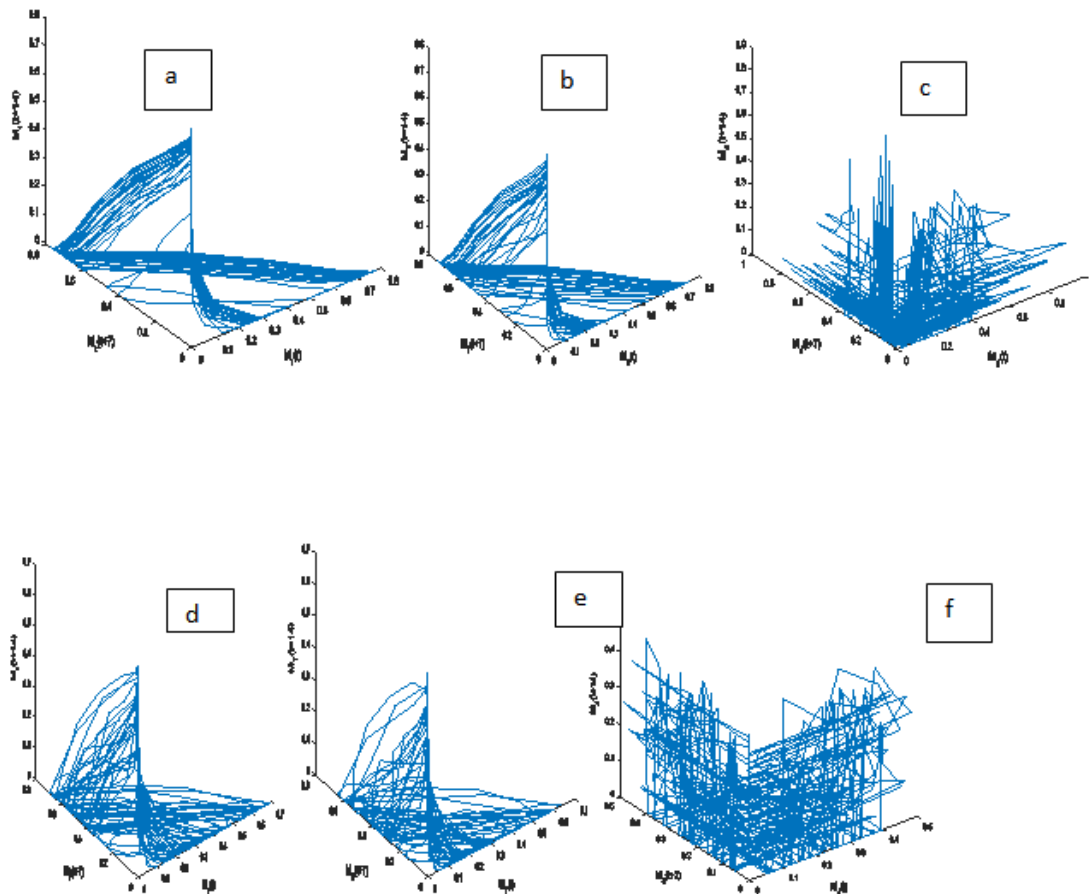


Figure 3: Typical phase plots for:
 Dry season: (a) M_t (b) M_T (c) M_d
 Wet season: (d) M_t (d) M_T (e) M_d

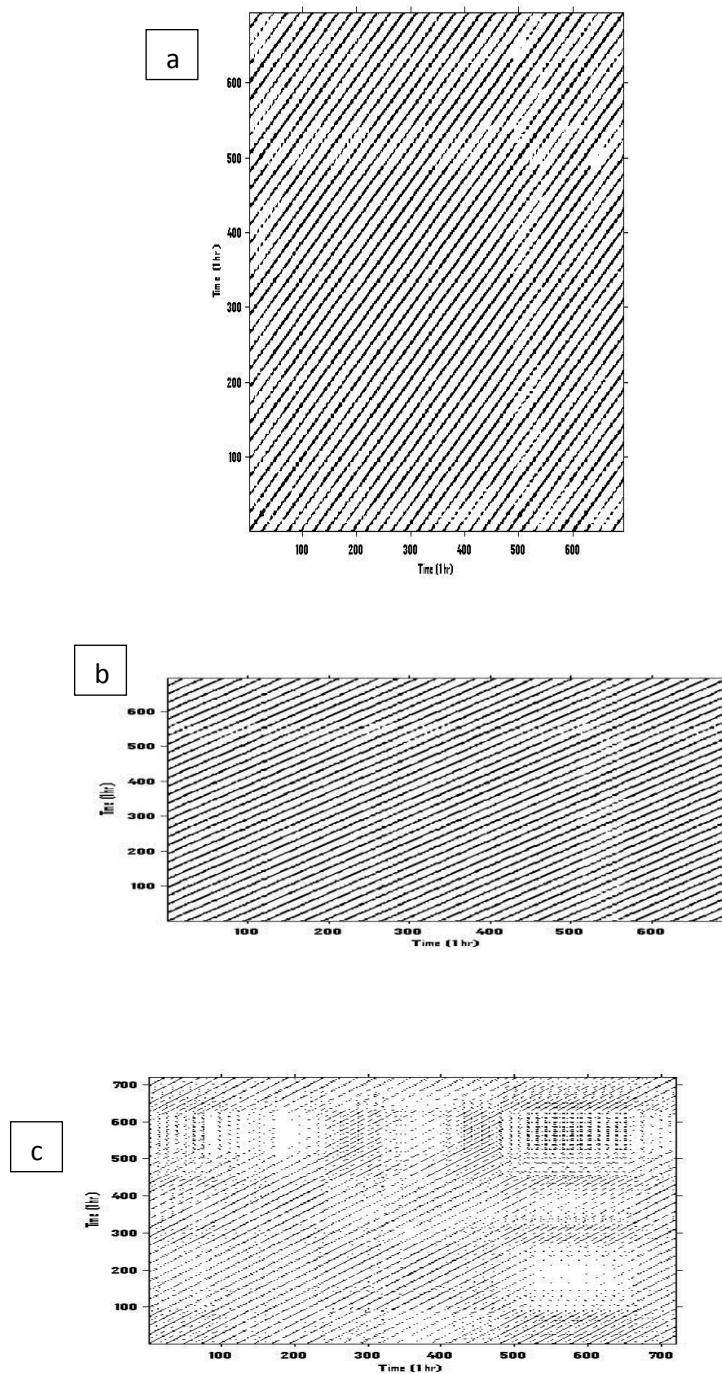


Figure 4: Typical recurrence plots for (a) M_t (b) M_T (c) M_d

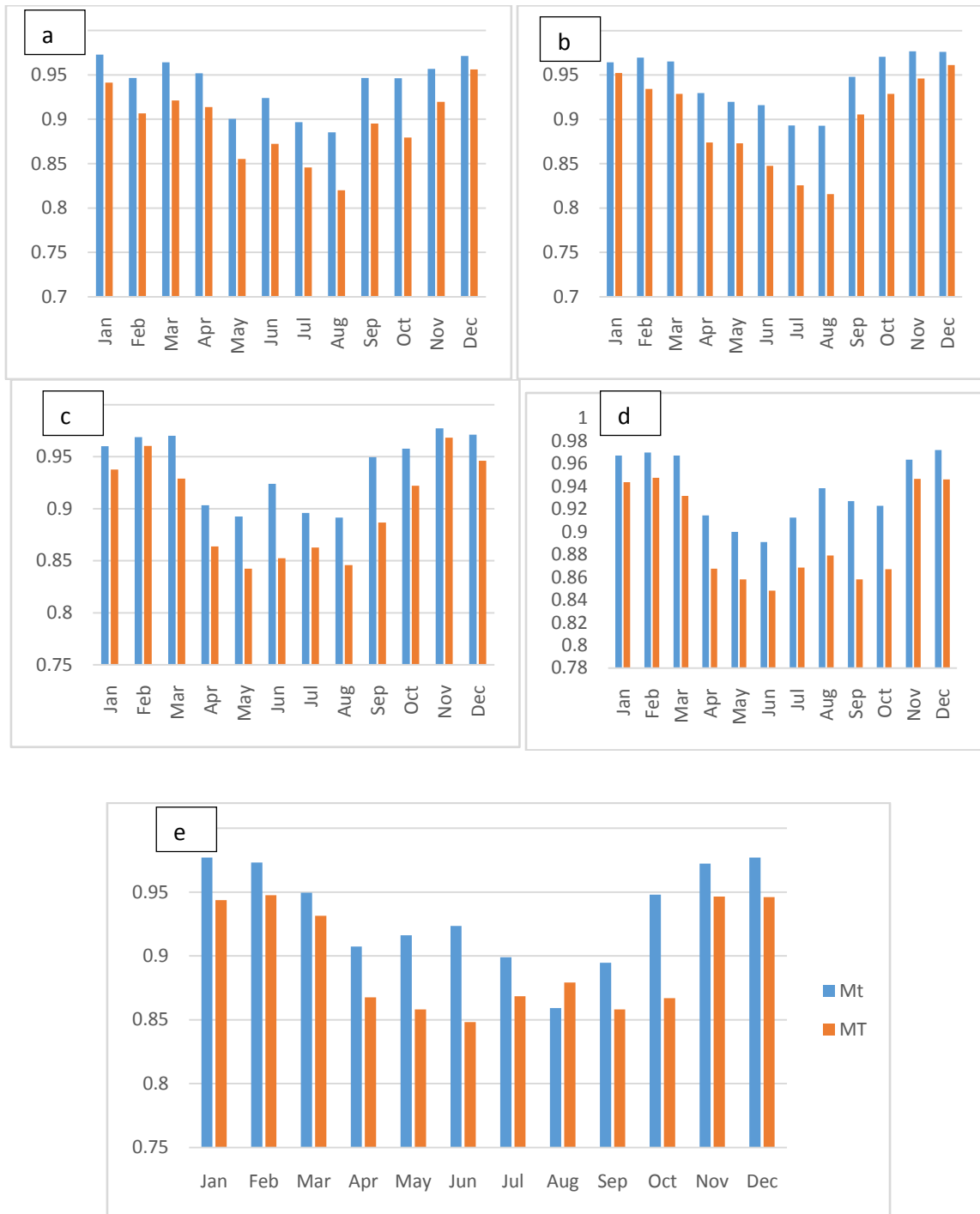


Figure 5: Determinism for (a) 2006 (b) 2007 (c) 2008 (d) 2009 (e) 2010

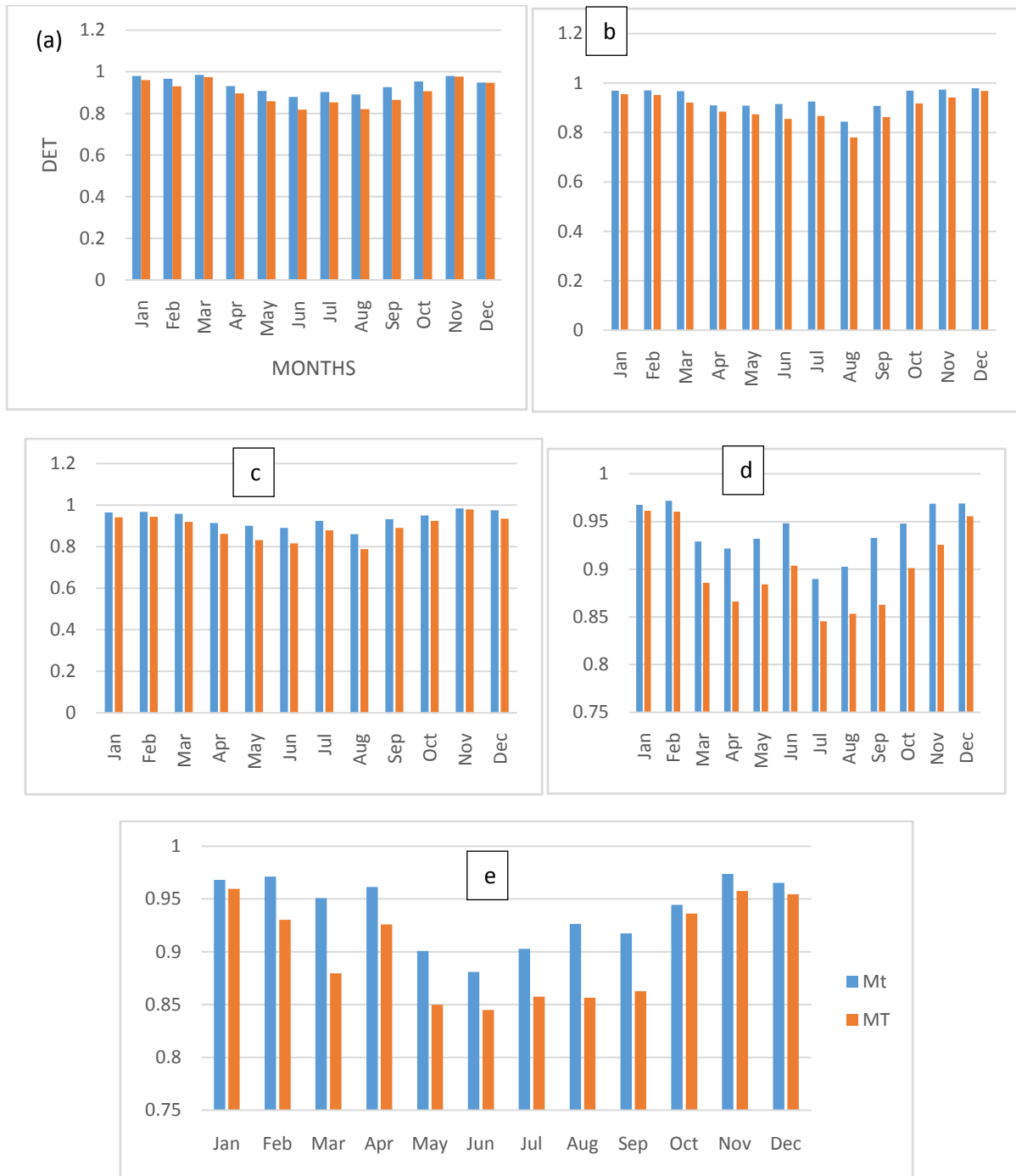


Figure 6: Determinism for (a) 2011 (b) 2012 (c) 2013 (d) 2014 (e) 2015

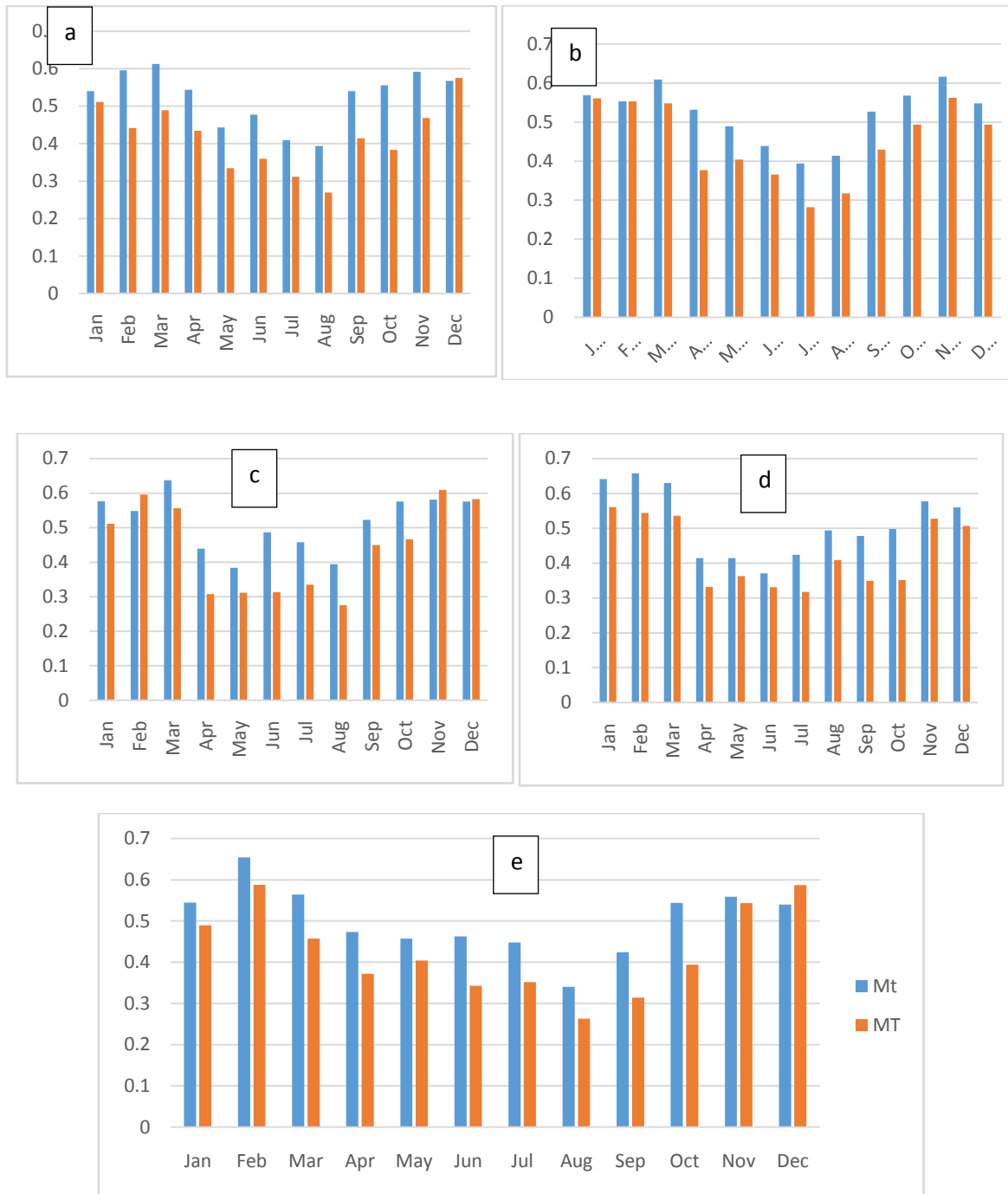


Figure 7: Entropy for (a) 2006 (b) 2007 (c) 2008 (d) 2009 (e) 2010



Figure 8: Entropy for (a) 2011 (b) 2012 (c) 2013 (d) 2014 (e) 2015

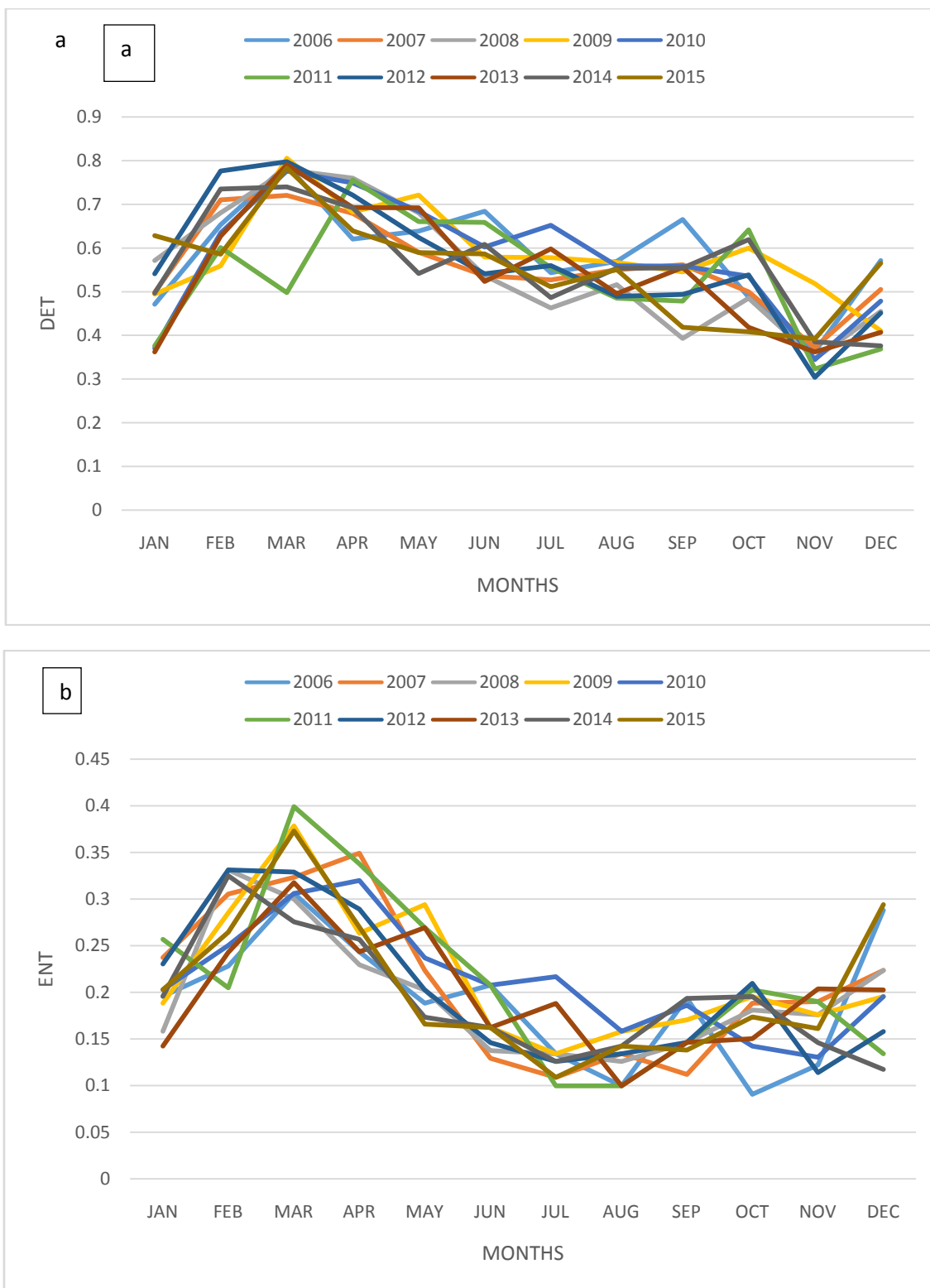


Figure 9: Plot of (a) Determinism (b) Entropy for M_d

Table 1: Yearly Maxima (MAX) and Minima (MIN) Determinism: (a) M_t (b) M_T (c) M_d

	YEAR	MAX	MONTH	MIN	MONTH
(a)	2006	0.972653	JAN	0.885399	AUG
	2007	0.976786	OCT	0.89273	AUG
	2008	0.977336	NOV	0.891517	AUG
	2009	0.971997	DEC	0.890942	JUN
	2010	0.976935	DEC	0.859209	AUG
	2011	0.984939	MAR	0.87973	JUN
	2012	0.97916	DEC	0.843548	AUG
	2013	0.984904	DEC	0.86037	AUG
	2014	0.971713	FEB	0.889783	JUL
	2015	0.973751	NOV	0.880967	JUN
(b)	YEAR	MAX	MONTH	MIN	MONTH
	2006	0.955978	DEC	0.819872	AUG
	2007	0.961381	DEC	0.815703	AUG
	2008	0.968261	NOV	0.842343	AUG
	2009	0.947548	FEB	0.848163	JUN
	2010	0.947548	FEB	0.848163	JUN
	2011	0.976634	NOV	0.81762	JUN
	2012	0.968319	DEC	0.780165	AUG
	2013	0.979357	NOV	0.788357	AUG
	2014	0.961143	JAN	0.845287	JUL
2015	0.959563	JAN	0.844946	JUN	
(c)	YEAR	MAX	MONTH	MIN	MONTH
	2006	0.790138	MAR	0.362486	NOV
	2007	0.720617	MAR	0.372298	NOV
	2008	0.778679	MAR	0.3472	NOV
	2009	0.805865	MAR	0.410517	DEC
	2010	0.776742	MAR	0.344414	NOV
	2011	0.75586	APR	0.323052	NOV
	2012	0.79803	MAR	0.303836	NOV
	2013	0.790806	MAR	0.362415	NOV
	2014	0.739912	FEB	0.37609	DEC
2015	0.783301	MAR	0.391883	NOV	

References

- [1]. Hegger R., Kantz, H. and Shreiber, T., (1994): Practical implementation of nonlinear time series method. The Tisean package, *Chaos*, 9, 413 – 430.
- [2]. Unnikrishnan, K., (2010): Comparative study of chaoticity of Equatorial/low latitude ionosphere over Indian subcontinent during geomagnetically quiet and disturbed periods. *Non Linear Processes in Geophys*, 26, 941-953.
- [3]. Sopian K., Alghout M.A., Alfegi E. M., Sulaiman M. Y., and Musa E A. (2009): Evaluation of thermal efficiency of double-pass solar collector with porous-nonporous media. *Renewable Energy*, 34: 640-645
- [4]. Ideriah F. J. K. and Suleman S. O. (1989) Sky conditions at Ibadan during 1975–1980. *Solar Energy* **43**, 325–330.
- [5]. Liu B. Y. U. and Jordan R. C. (1960) The inter-relationship and characteristic distribution of direct, diffuse and total solar radiation. *Solar Energy* **4**, 1–19.
- [6]. Choudhury N. K. D. (1963) Solar radiation at New Delhi. *Solar Energy* **7**, 44.
- [7]. Barbaro S., Cannata G., Coppilino S., Leone C. and Sinagra E. (1981) Diffuse radiation statistics for Italy. *Solar Energy* **26**, 429–435.
- [8]. Al-Riahi M., Al-Hamdani N. and Tahir T. (1990) Contribution to the study of solar radiation climate of Baghdad environment. *Solar Energy* **44**, 7–12.
- [9]. Akuffo F. O. and Brew-Hammond A. (1993) The frequency distribution of global solar irradiation at Kumasi. *Solar Energy* **50**, 145–154.
- [10]. Ezekwe, C.I. and Clifford, Ezeilo C.O. (1981): Measured solar radiation in a Nigerian environment compared with predicted data. *Solar Energy* Volume 26, Issue 2, Pages 181-186.
- [11]. Knut Stamnes and Jakob J. Stamnes, Transport of Solar Radiation through the Atmosphere: Aspects Relevant for Health; In: *Solar Radiation and Human Health* Espen Bjertness, editor. Oslo: The Norwegian Academy of Science and Letters, 2008.
- [12]. Babatunde, E. B. (2005): Some solar radiation ratios and their interpretations with regards to radiation transfer in the atmosphere. *Nig. J. of Pure & Appl. Physics*. Vol. 4. Pages 41– 45, 2005.
- [13]. Okogbue, E.C., Adedokun, J.A. and Holmgren, B. (2009): Hourly and daily clearness index and diffuse fraction at a tropical station, Ile-Ife, Nigeria. *International Journal of Climatology* **29**, 1035 -1047.
- [14]. Ndilemeni C. C., Momoh and J.O. Akande "Evaluation of Clearness Index of Sokoto Using Estimated Global Solar Radiation" *IOSR Journal Of Environmental Science, Toxicology And Food Technology (IOSR-JESTFT)*
- [15]. Yusuf, A. (2017): Characterization of sky conditions using clearness index and relative sunshine duration for Iseyin, Nigeria. *International Journal of Physical Sciences Research*, Vol.1, No.1, 53-60.
- [16]. Udo S. O. and Aro T. O. (1999) Measurement of global solar, global photosynthetically active and downward infrared radiations at Ilorin, Nigeria. *Renewable Energy* **17**, 113– 122
- [17]. Okogbue E. C., Adedokun J. A. 2002. Characterization of sky conditions over Ile-Ife, Nigeria based on 1992–1998 Solar Radiation Observations. *Meteorologische Zeitschrift, Germany* **11**(6): 419–423.
- [18]. Takens F., (1981): Detecting strange attractors in turbulence: Lecture notes in mathematics, vol. 898, no. 1, 366-381.
- [19]. Kantz, H. and Shreiber, T., (2003): *Nonlinear time series analysis*, second ed. Cambridge University Press.
- [20]. Fraser A.M. and Swinney H.L., (1986): Independent coordinates for strange attractors from mutual information. *Phys. Rev. A*, **33**, 1134 – 1141.
- [21]. Poincare J. H. (1885): *The three-body problem and the equations of dynamics: Poincare's foundational work on dynamical systems theory*. Cham, Switzerland: Springer International Publishing. ISBN 9783319528984
- [22]. Abarbanel H. D., Brown R., Sidorowich J. J., and Tsimring L. S., (1993): The analysis of observed chaotic data in physical systems. *Reviews of modern physics*, vol. 65, no. 4, 1331.
- [23]. Eckmann, J. P., Kamphorst, S. and Ruelle, D., (1987): Recurrence plots of dynamical systems. *Europhys. Lett.* **4**, 973–977.
- [24]. Thiel, M., Romano, M. C., Kurths, J., Meucci, R., Allaria, E., and Arecchi, F. T., (2002):
- [25]. Influence of observational noise on the recurrence quantification analysis. *Physica D* **171**, 138–152.
- [26]. Marwan, N., (2003): Encounters with neighbours: Current development of concepts based on recurrence plots and their applications. Ph.D. Thesis, Universität Potsdam, pp. 18–21.
- [27]. Zbilut, J. and Webber, J. C. (1992): Embeddings and delays as derived from quantification of recurrence plots. *Physics Letters A* **171**, 199–203 (1992). (Taylor & Francis Group).
- [28]. Webber, C. L. and Zbilut, J. P., (1994): Dynamical assessment of physiological systems and states using recurrence plot strategies. *Journal of Appl. Physiol.* **76**, 965–973.
- [29]. Trulla, L. L., Giuliani, A., Zbilut, J. P., and Webber, Jr., C. L., (1996): Recurrence quantification analysis of the logistic equation with transients. *Physics Letters A* **223**, 255–260.
- [30]. Shannon, C. E., (1948): A mathematical theory of communication. *Bell Systems Technical Journal* **27**, 379–423 and 623–656
- [31]. Kennel, M.B., Brown, R., and Abarbanel, H.D.I., (1992): Determining minimum embedding dimension using a geometrical construction. *Phys. Rev. A*, **45**, 3403 – 3411.
- [32]. Marwan, N., (2010): Cross recurrence plot toolbox 5.21 (R31), <http://www.agnld.uni-potsdam.de/~marwan/toolbox>.
- [33]. Wallot, S., (2017): Recurrence quantification analysis of processes and products of discourse: A tutorial in R. *Discourse Processes* (Taylor & Francis group)
- [34]. Adeyemi B. and Ogolo E.O., (2014): Diurnal and seasonal variations of surface water vapor density over some meteorological stations in Nigeria. *Ife Journal of Science* vol. 16, no. 2, 127-169
- [35]. Schinkel, S., Dimigen, O., and Marwan, N., (2008): Selection of recurrence threshold for signal detection. *European Physical Journal – Special Topics* **164**, 45–53.
- [36]. Iqbal M. (1983). *An Introduction to Solar Radiation*, Academic Press, Toronto.
- [37]. Marwan, N., Romano, M. C., Thiel, M., and Kurths, J., (2007): Recurrence plots for the analysis of complex systems, *Phys. Rep.* **438**, 237–329.
- [38]. Webber, C. L. and Zbilut, J. P., (2005): Recurrence Quantification Analysis of Nonlinear Dynamical Systems. <http://www.nsf.gov/sbe/bcs/pac/nmbs/nmbs.jsp>

O. V. EDWARD. " Comparative Study of Some Atmospheric Transmittance Indices over Jos Using Recurrence Quantification Analysis" *IOSR Journal of Applied Physics (IOSR-JAP)* , vol. 11, no. 4, 2019, pp. 40-57.